Nuclear expansion with excitation

J. N. De[1,2], S. K. Samaddar[1], X. Viñas[2], and M. Centelles[2]

[1]*Saha Institute of Nuclear Physics,*

1/AF Bidhannagar, Kolkata 700064, India

[2]*Departament d'Estructura i Constituents de la Matèria, Facultat de Física,*

Universitat de Barcelona, Diagonal 647, 08028 Barcelona, Spain

Abstract

The expansion of an isolated hot spherical nucleus with excitation energy and its caloric curve are studied in a thermodynamic model with the SkM* force as the nuclear effective two-body interaction. The calculated results are shown to compare well with the recent experimental data from energetic nuclear collisions. The fluctuations in temperature and density are also studied. They are seen to build up very rapidly beyond an excitation energy of ~ 9 MeV/u. Volume-conserving quadrupole deformation in addition to expansion indicates, however, nuclear disassembly above an excitation energy of ~ 4 MeV/u.

PACS numbers: 25.70.Pq, 25.70.Gh

Keywords: caloric curve; break-up density; nuclear expansion; hot nuclei

Understanding the density evolution of nuclear systems at moderate excitation energies ($\sim 2-8$ MeV/u) is of much contemporary interest, both from the theoretical and the experimental point of view. This is particularly relevant in the context of nuclear multi-fragmentation at intermediate energy heavy ion collisions [1, 2, 3]. With excitation, the thermal pressure pushes the system towards expansion. At sufficiently high excitations, the system is ultimately driven towards the *break-up* density below which it ceases to exist in a mononuclear configuration and ultimately disassembles into many fragments. This has an important bearing in modelling the equation of state [4] of hot nuclear systems; it is also of utmost importance in understanding explosive nucleosynthesis [5, 6] in the astrophysical context.

Experimental studies have been suggestive of decreasing break-up density with increasing excitation energy. Break-up densities have been determined from studies of correlation functions of emitted light particles from the source [7]. It is found that this density in general decreases with increasing excitation energy in the fragmenting system, however, the method of analysis leaves room for large uncertainties. QMD transport model calculations indicate that for medium-heavy systems, for excitation energy less than ~ 7 MeV/u, densities as low as $\sim 0.35\rho_0$ can be reached [8] where ρ_0 is the ground state density. Break-up densities have also been determined from Coulomb barriers required to fit the intermediate mass ejectile spectra [9, 10]; they have as well been determined from the analysis of apparent level density parameters required to fit the measured caloric curves [11]. At an excitation energy of ~ 8 MeV/u, the deduced density comes down to $\sim 0.3-0.4\,\rho_0$, but in the excitation energy range explored, the last two sets of results are not exactly in consonance; break-up densities derived from Coulomb barrier systematics are lower at higher excitations compared to those derived from caloric curve data.

From a theoretical standpoint, statistical models [1, 2, 3] have been quite successful in explaining various observables related to nuclear fragmentation. The key parameter in these models is the *freeze-out* density ρ_f. On reaching ρ_f, the hot nucleus undergoes one-step prompt multifragmentation and the interaction among the generated fragments is assumed to be frozen out to change the fragmentation pattern. The freeze-out density is generally taken to be independent of the excitation energy. This density differs appreciably in different models. Whereas in the canonical or microcanonical models proposed in Refs. [1, 2], the density ρ_f is $\sim 0.12-0.2\,\rho_0$, the corresponding density in the lattice-gas model [12, 13]

is $\sim 0.3 - 0.4\,\rho_0$. Such an uncertainty in both the theoretical and the experimental arena warrants a closer look at the relationship of the nuclear density with excitation energy. To explore the break-up density of a hot metastable mononuclear configuration, Sobotka *et al* [14] have recently performed a calculation where they utilise the fact that an isolated system with a given excitation energy pursues the maximal entropy configuration for equilibrium. This calculation is schematic and involves a few *ad hoc* parameters; the results compare favorably with the data reported in Ref. [11]. In the present communication, we address this problem with some basic microscopic inputs starting with a Skyrme type effective two-body interaction. We use the celebrated SkM* force [15], well known for its success in the description of a variety of ground-state properties of nuclei and diverse phenomena like nuclear fission and nuclear collective modes.

The experimental perspective in the laboratory is recalled briefly. When two nuclei collide at intermediate energy, a hot nuclear system (which may be initially somewhat compressed; the possible resulting collective flow is ignored in this work) is formed which may be described statistically by an effective temperature T. If the system were in a heat bath at the temperature T (canonical ensemble), the system could be described by equilibrium thermodynamics driving it to the minimum of the free energy. However, the system as prepared, is isolated with a fixed total excitation energy (microcanonical ensemble). The unbalanced thermal pressure induces expansion of the system in search of maximal entropy where the total pressure vanishes and the system is in equilibrium in a mononuclear configuration. The energy of expansion is derived from the thermal energy, the temperature thereby decreases. The density at this maximal entropy state is the lower limit (break-up density) for a mononuclear configuration with a fixed excitation energy. The system may, however, gain further entropy from nuclear disassembly. A full-fledged study of the nuclear disassembly path is not taken up here, it is mimicked through a volume conserving deformation of the system at the various stages of expansion. For simplicity, we consider only quadrupole deformation.

The initial state of the system is prepared by subjecting it in a heat bath at a chosen temperature T. Employing the SkM* interaction [15], this is done in a finite temperature Thomas-Fermi framework within the subtraction scheme [16, 17], well suited for the description of hot nuclei. The system so prepared is then detached from the heat bath and allowed to expand with constant total energy in pursuit of the maximal entropy state. The

expansion is simulated through a self-similar scaling approximation for the density:

$$\rho_\lambda(r) = \lambda^3 \rho(\lambda r)\,, \tag{1}$$

where the scaling parameter λ lies in the range $0 < \lambda \leq 1$ and $\rho(r)$ is the base density profile generated in the Thomas-Fermi procedure.

In actual calculations, we first fix the total excitation energy E^*. The base density profile of the system is generated at a chosen temperature T such that the excitation energy for this density profile is less than the given E^*. The system is then allowed to undergo a self-similar expansion till the total excitation energy (thermal plus expansion) reaches E^* at some value of $\lambda < 1$. For any density profile, the excitation energy is calculated as

$$E^* = E(\lambda, T) - E(\lambda = 1, T = 0) \tag{2}$$

from the Skyrme energy density functional [15]. The corresponding entropy for the expanded configuration $S(\lambda, T)$ is computed. The calculations are repeated for different T; the configuration corresponding to the maximum of the entropy profile $S(\lambda, T)$ is the desired equilibrium configuration at the energy E^*.

In the subtraction procedure [16, 17] the base density for the hot nucleus is given by $\rho(r) = \rho_{ng}(r) - \rho_g(r)$, where $\rho_g(r)$ is the density of the surrounding gas representing evaporated nucleons in which the system is immersed to maintain equilibrium at the temperature T and $\rho_{ng}(r)$ is the density of the nucleus-plus-gas system. The density profile $\rho(r)$ of the heated nucleus is then independent of the size of the box in which calculations are done, the density and pressure being zero at large distances. In the Thomas-Fermi method, the densities $\rho_i(r)$ for neutrons or protons (i stands for ng or g) are given by

$$\rho_i(r) = \frac{1}{2\pi^2}\left[\frac{2m_i^*(r)}{\hbar^2}\right]^{\frac{3}{2}} \int_{V_i(r)}^{\infty} \sqrt{\varepsilon - V_i(r)}\, f(\varepsilon, \mu, T)\, d\varepsilon. \tag{3}$$

Here $m_i^*(r)$ is the effective k-mass of the nucleon, $V_i(r)$ is the single-particle potential, f is the Fermi occupation factor, and μ is the chemical potential which is same in both the ng and g phases. The effective mass, single-particle potential, and the chemical potential are isospin dependent. The chemical potentials are determined from particle number conservation (N is the neutron or proton number):

$$N = \int g(\varepsilon, T) f(\varepsilon, \mu, T) d\varepsilon, \tag{4}$$

where the single-particle level density $g(\varepsilon, T)$ of the hot nucleus in the subtraction procedure is given by [17]

$$g(\varepsilon, T) \;=\; \frac{4\sqrt{2}}{\pi\hbar^3} \int \left[(m^*_{ng})^{\frac{3}{2}} \sqrt{\varepsilon - V_{ng}(r)} - (m^*_g)^{\frac{3}{2}} \sqrt{\varepsilon - V_g(r)} \right] r^2 dr. \tag{5}$$

The effective mass, single-particle potential, and the chemical potential are evaluated at the appropriate temperature and scaled densities, so also the single-particle level density and the entropy. The latter reads as

$$S(\lambda, T) = -\int g(\varepsilon, T) \left[f \ln f + (1-f) \ln(1-f) \right] d\varepsilon. \tag{6}$$

The total entropy is the sum of the neutron and proton contributions.

For our study, we have chosen ^{150}Sm as a representative system. The central density ρ_c of the calculated mononuclear equilibrium configuration in units of ρ_0 (the central density of the unexpanded nucleus at $T = 0$) [18] is displayed in Fig. 1 as a function of the excitation energy and compared with the experimental data. The thin (dashed and solid) lines correspond to the canonical ensemble calculations, *i.e.*, when the system is in a heat bath; the thick lines are those for the isolated expanded nucleus at equilibrium. The filled circles are the experimental points extracted from the apparent level density parameters [11] for the mass selection $140 < A < 180$, where A is the mass number of the system, and the empty squares are the ones obtained from Coulomb barrier systematics [9, 10] for Au-like systems.

The effective mass m^* defined previously comes from the momentum dependence of the single-particle potential, which is the k-mass m_k. However, m^* should have a frequency dependent mass-factor m_ω/m:

$$m^* = m \frac{m_k}{m} \frac{m_\omega}{m}. \tag{7}$$

The ω-mass originates from the coupling of the single-particle motion with the collective degrees of freedom. This has the effect of bringing down the excited states from high energy to lower energy near the Fermi surface, thus increasing the many-body density of states [$m_\omega/m \geq 1$, see Eq. (8)] at low excitations. It may *a priori* have a significant role to play in the present context as the system can accommodate comparatively more entropy at a given excitation energy. The self-consistent evaluation of the ω-mass is beyond the scope of the present work; we use the phenomenological form [19, 20]

$$\frac{m_\omega}{m} = 1 - 0.4\, A^{\frac{1}{3}} \exp\left[-\left(\frac{T}{21 A^{-\frac{1}{3}}} \right)^2 \right] \frac{1}{\rho(0)} \frac{d\rho(r)}{dr}, \tag{8}$$

where $\rho(r)$ is the density profile at temperature T. The effect of m_ω is incorporated [19, 21] by replacing the single-particle potential V with $(m/m_\omega)V$ in Eqs. (3)–(5).

In Fig. 1, the solid (dashed) lines refer to calculations performed with (without) inclusion of m_ω/m. With increasing temperature, m_ω/m tends to unity. We find that the values of ρ_c calculated at moderate or higher excitations with and without the inclusion of the ω-mass are practically the same; however, the relative densities ρ_c/ρ_0 for the two cases run parallel there because the values of ρ_0 are different in the two situations. The calculations for the canonical ensemble (thin lines) terminate at an excitation energy of ~ 5.5 MeV/u corresponding to $T \simeq 8.5$ MeV, the limiting temperature [16, 17] for this nucleus beyond which it is unstable in a heat bath. The thick curves, as compared to the thin ones, show appreciably lower values of density that compare reasonably with the densities extracted from the analysis of the caloric curve measurements performed in [11] (filled circles). The importance of a microcanonical treatment is thereby indicated. The fit with the data obtained from Coulomb barrier systematics (filled squares) [10] is relatively poor; however, an ambiguity in their extraction procedure has been pointed out recently [22].

The ω-mass does not appear to have a very distinctive role to the density evolution with excitation energy. In the excitation range indicated in the figure, it turns out that with inclusion of the ω-mass, the equilibrium configuration corresponds to a lower value of the temperature as compared to that obtained with m_ω/m=1; this tends to increase the central density ρ_c in the former case. On the other hand, the scale parameter λ is found to be comparatively lower with inclusion of the ω-mass, resulting in a lower value of ρ_c. The combined effect of these opposing tendencies then results in the near equality of ρ_c in both the calculations.

The expansion of the nucleus has an important bearing on the correlation of the excitation energy with temperature. The caloric curve so obtained for the expanded hot nucleus ^{150}Sm in equilibrium is displayed in the upper panel of Fig. 2. At a fixed excitation energy, the system cools down with expansion and therefore the recorded temperature at the equilibrium configuration is significantly lower than that for the unexpanded nucleus prepared initially with the same excitation. In the figure, T refers to the canonical temperature. We have checked that the microcanonical temperature obtained from $T^{-1} = \partial S_{\rm eq}/\partial E^*$, where $S_{\rm eq}$ is the total entropy and E^* the excitation energy at equilibrium, is not much different from the canonical one. For comparison, a representative set of experimental data for medium

mass nuclei [8] are also shown in the figure. The notations used have the same meaning as in Fig. 1. The effect of isolation is not appreciable at relatively lower excitations, but is more manifest at higher excitations. The calculated microcanonical results are seen to agree nicely with the experimental caloric curve. The canonical caloric curves with and without the inclusion of the ω-mass merge at high temperatures because m_ω/m does not differ much from unity. The microcanonical caloric curves, on the other hand, even at high excitations do not merge; the highest temperature encountered in these calculations is ~ 8 MeV where m_ω/m is typically ~ 1.02 at the surface region affecting the equilibrium configuration a little which is amplified in the caloric curve.

At a given temperature, the system is found to have more excitation with inclusion of the ω-mass as more states are available near the Fermi surface to absorb more energy. Beyond $E^*/A \sim 6$ MeV, T seems to saturate and at $E^*/A \sim 8$ MeV, a downward slope in the caloric curve is apparent for the isolated system implying negative heat capacity. The expansion energy $[E_{\rm expn} = E(\lambda, T) - E(\lambda = 1, T)]$ comprises a significant part of the total excitation at higher values of E^* inducing the above-mentioned characteristics in the caloric curve. The expansion energy is found to be in good agreement with that obtained in the Expanding Emitting Source model of Friedman [23] as shown in the lower panel of Fig. 2. The filled diamond refers to an experimental estimate [10], which is close to the prediction from our calculations.

The entropy profile obtained at a fixed excitation energy may be employed to calculate the mean values and the fluctuations around the mean of the temperature and of the density or volume. The probability of finding a configuration with scale parameter λ and temperature T at a fixed excitation energy E^*/A is given by

$$W(\lambda, T) \propto e^{S(\lambda,T)} \ , \tag{9}$$

where $S(\lambda, T)$ is the total entropy (6) of the given configuration. The n-th moment of the central density ρ_c is then given by

$$\langle \rho_c^n(\lambda, T) \rangle = \frac{\int e^{S(\lambda,T)} \rho_c^n(\lambda, T) d\rho}{\int e^{S(\lambda,T)} d\rho} \ , \tag{10}$$

which allows to calculate the mean $\langle \rho_c \rangle$ and the variance $\sigma_\rho^2 = \langle \rho_c^2 \rangle - \langle \rho_c \rangle^2$. Similarly, the mean and variance of the temperature at a fixed excitation can be evaluated.

For a thermodynamic system, the average and the most probable (equilibrium) value of an observable are the same. For a finite system, however, they may be different. Experimentally,

the average value is the relevant quantity. The average and the most probable values of the temperature and the specific volume v_c ($= 1/\rho_c$) in units of v_0 ($= 1/\rho_0$) for the system considered are displayed in the upper and lower panels of Fig. 3. It is seen that the differences between the averages and the most probable values of the temperature and the break-up volume (or density) are not very significant. The fluctuations σ^2 in temperature and the specific volume (measured in units of v_0) are shown in Fig. 4. The fluctuations rise smoothly up to the excitation energy $E^*/A \sim 9$ MeV, beyond which this build-up is very sudden; this is particularly more pronounced for the volume fluctuations. This large density fluctuation indicates that beyond $E^*/A \sim 9$ MeV the system becomes unstable and breaks up in many pieces. It turns out that the negative branch of the specific heat (Fig. 3) and the large fluctuations start at around the same excitation energy. A possible close correlation between them is thereby indicated.

So far, for the search of the maximum entropy configuration, the shape of the excited expanding system has been constrained to a spherical one; a possible deformation path along with expansion might also contribute additional entropy and mimics a fragmentation channel. To investigate this aspect, at all stages of the expansion at a fixed excitation energy, a volume conserving quadrupole deformation is explored. In a volume conserving deformation, only the surface and Coulomb energies change. To calculate these changes, a sharp surface approximation to the density profile is made ($R_{\rm sharp} = \sqrt{\frac{5}{3}\langle r^2\rangle}$) which also facilitates the calculation of entropy from deformation. At a deformation β, the excess Coulomb energy of the expanded deformed nucleus is $\delta E_c(\lambda,\beta) = E_c(\lambda,0)f(\beta)$; the function $f(\beta)$ is given in Ref.[24]. The surface free energy due to deformation is given by $\delta F(\lambda,\beta) = \delta\mathcal{A}(\lambda,\beta)\sigma(\rho,T)$, where $\delta\mathcal{A}$ is the excess surface area of the nucleus arising out of deformation. The surface tension coefficient σ at a density ρ and temperature T is taken as $\sigma(\rho,T) = \alpha(T)g(\rho)$. The temperature dependence [25] of the surface tension is given by $\alpha(T)$. The surface tension has its maximum value at the ground-state density; for an expanded system, σ decreases which can be well represented by $g(\rho)$ taken to be a polynomial in ρ. We have calculated this density dependence from the prescription of Myers and Swiatecki [26] using the scaling approximation to the ground-state density profile of semi-infinite nuclear matter. The excess entropy from deformation is then calculated as $\delta S = -\partial(\delta F)/\partial T|_\rho$ which immediately gives the excess surface energy $\delta E_{\rm surf} = \delta F + T\delta S$. The total excitation energy of the expanded deformed system is then $\mathcal{E}^*(\lambda,\beta) = \mathcal{E}^*(\lambda,0) + \delta E_c(\lambda,\beta) + \delta E_{\rm surf}(\lambda,\beta)$

and the corresponding entropy is $S(\lambda,\beta) = S(\lambda,0) + \delta S(\lambda,\beta)$.

Along the deformation path, a barrier is faced coming from the interplay of the Coulomb and surface energies; it decreases with increasing temperature and increasing expansion. In actual calculations, the scale parameter λ is adjusted such that for a chosen temperature, the excitation energy at the top of the barrier $\mathcal{E}^*(\lambda,\beta)$ matches the given excitation E^*/A. This is repeated for different temperatures and the maximum entropy among these different configurations is selected. If this entropy exceeds that for the expanded spherical equilibrium configuration, then the deformed shape is favoured leading to the fragmentation channel.

This extra entropy gained due to deformation (we call this ΔS) over that at the spherical equilibrium shape is shown in the top panel of Fig. 5 as a function of excitation energy. For E^*/A less than $\sim$ 4 MeV, ΔS is negative in our chosen restricted deformation space and so a spherical equilibrium configuration is more probable. Above this excitation energy, fragmentation resulting from deformation is more favourable. Beyond $E^*/A \sim 9$ MeV, the barrier vanishes and the system undergoes spontaneous fragmentation from the spherical equilibrium configuration.

In the middle panel of Fig. 5, the equilibrium central densities with (solid line) and without (dashed line) deformation are displayed as a function of E^*/A. With deformation, the maximal entropy configuration occurs at a lower temperature with a smaller scale parameter λ resulting in a somewhat reduced density as seen. The corresponding caloric curves are shown in the bottom panel. All the above calculations pertain to prolate deformation, oblate shapes are found to have lesser entropy.

We have addressed to some gross features of a mononuclear configuration at medium and high excitations in a semi-microscopic framework based upon a realistic effective nuclear interaction. The calculated break-up densities for the nucleus in the microcanonical formulation are in general in good agreement with the ones extracted from the experimental data analysis [11]. The generated mononuclear caloric curve also compares very well with the experimental results. The plateau observed in experimental data has been taken to be suggestive of a possible phase coexistence [27]. In our calculations, the plateau comes naturally from nuclear expansion with excitation. For the bloated spherical mononuclear configuration, the rapid build-up of fluctuations, particularly in the density, is suggestive of the instability of this configuration against prompt multifragmentation beyond $E^*/A \sim 9$ MeV. Expansion with deformation degrees of freedom may have significant effects on the

physical observables; to have an orientation on the role of deformation, we have considered volume-conserving quadrupole deformation. It is found that above $E^*/A \sim 4$ MeV the system favours deformation, a precursor to fragmentation. The global trends provided by the present model, particularly with the inclusion of the frequency dependence in the effective mass, are qualitatively consistent with the experimental data [9, 10, 11] as well as with the ones obtained from other mononuclear formulations [14, 28]. At high excitations, the collective flow may play a significant role in the nuclear collision process. This has been ignored in the present calculation; it would be worthwhile to investigate its effect on the break-up density and also on the caloric curve.

J.N.D. and S.K.S. acknowledge the financial support from DST and CSIR, Government of India, respectively. J.N.D. gratefully acknowledges the hospitality at the University of Barcelona and a financial grant 2003PIVB00077 from Generalitat de Catalunya. M.C. and X.V. acknowledge financial support from Grants No. FIS2005-03142 from MEC (Spain) and FEDER, and No. 2005SGR-00343 from Generalitat de Catalunya.

---

[1] J. P. Bondorf *et al*, Phys. Rep. 257 (1995) 133.

[2] D. H. E. Gross, Rep. Prog. Phys. 53 (1990) 1122.

[3] Ph. Chomaz, M. Colonna, and J. Randrup, Phys. Rep. 389 (2004) 263.

[4] H. Stocker and W. Greiner, Phys. Rep. 137 (1986) 277.

[5] C. Ishizuka, A. Ohnishi, and K. Sumiyoshi, Nucl. Phys. A723 (2003) 517.

[6] A. S. Botvina and I. N. Mishustin, Phys. Lett. B584 (2004) 233.

[7] S. Fritz *et al*, Phys. Lett. B461 (1999) 315.

[8] J. Cibor *et al*, Phys. Lett. B473 (2000) 29.

[9] D. S. Bracken *et al*, Phys. Rev.C 69 (2004) 034612.

[10] V. E. Viola *et al*, Phys. Rev. Lett. 93 (2004) 132701.

[11] J. B. Natowitz *et al*, Phys. Rev.C 66 (2002) 031601(R).

[12] S. Das Gupta and J. Pan, Phys. Rev.C 53 (1996) 1319.

[13] Ph. Chomaz and F. Gulminelli, Phys. Lett. B447 (1999) 221.

[14] L. G. Sobotka *et al*, Phys. Rev. Lett. 93 (2004) 132702.

[15] M. Brack, C. Guet, and H.-B. Håkansson, Phys. Rep. 123 (1985) 275.

[16] P. Bonche, S. Levit, and D. Vautherin, Nucl. Phys. A436 (1985) 265.

[17] E. Suraud, Nucl. Phys. A462 (1987) 109.

[18] Since the density has a profile, the use of a single value for ρ has some room for ambiguity. To keep ρ_c and ρ_0 on the same footing, we have taken for ρ_0 the value of the ground-state central density. It has, however, been checked that the results are nearly insensitive to the choice of ρ as the corresponding equivalent uniform density at the relevant temperatures.

[19] M. Prakash, J. Wambach, and Z. Y. Ma, Phys. Lett. B128 (1983) 141.

[20] S. Shlomo and J. B. Natowitz, Phys. Lett. B252 (1990) 187.

[21] J. N. De, S. Shlomo, and S. K. Samaddar, Phys. Rev. C 57 (1998) 1398.

[22] Ad. R. Raduta *et al*, Phys. Lett. B623 (2005) 43.

[23] W. A. Friedman, Phys. Rev. Lett. 60 (1988) 2125.

[24] J. M. Eisenberg and W. Greiner, *Microscopic Theory of the Nucleus* (North-Holland, Amsterdam, 1972), p. 395.

[25] J. P. Bondorf, R. Donangelo, I. N. Mishustin and H. Schulz, Nucl. Phys. A444 (1985) 460.

[26] W. D. Myers and W. J. Swiatecki, Ann. Phys. 55 (1969) 395.

[27] J. Pochodzalla *et al.*, Phys. Rev. Lett. 77 (1996) 235.

[28] L. G. Sobotka and R. J. Charity, Phys. Rev. C 73 (2006) 014609.

Figure Captions

Fig. 1 The calculated equilibrium density in units of ρ_0 as a function of the excitation energy per nucleon is compared with the experimental data. For notations, see text.

Fig. 2 The mononuclear caloric curve (upper panel) and the expansion energy per nucleon (lower panel).

Fig. 3 The average and the equilibrium values of temperature (upper panel) and the specific volume (lower panel) of the nucleus ^{150}Sm as a function of excitation energy.

Fig. 4 The variance in the temperature (upper panel) and the specific volume (lower panel) as a function of excitation energy.

Fig. 5 The deformation entropy ΔS (top panel), the equilibrium density in units of ρ_0 (middle panel) and the caloric curve (bottom panel). The solid lines represent the results with deformation and the dashed lines correspond to the spherical configuration. The experimental points (filled circles and open squares) are the same as those given in Figs. 1 and 2.

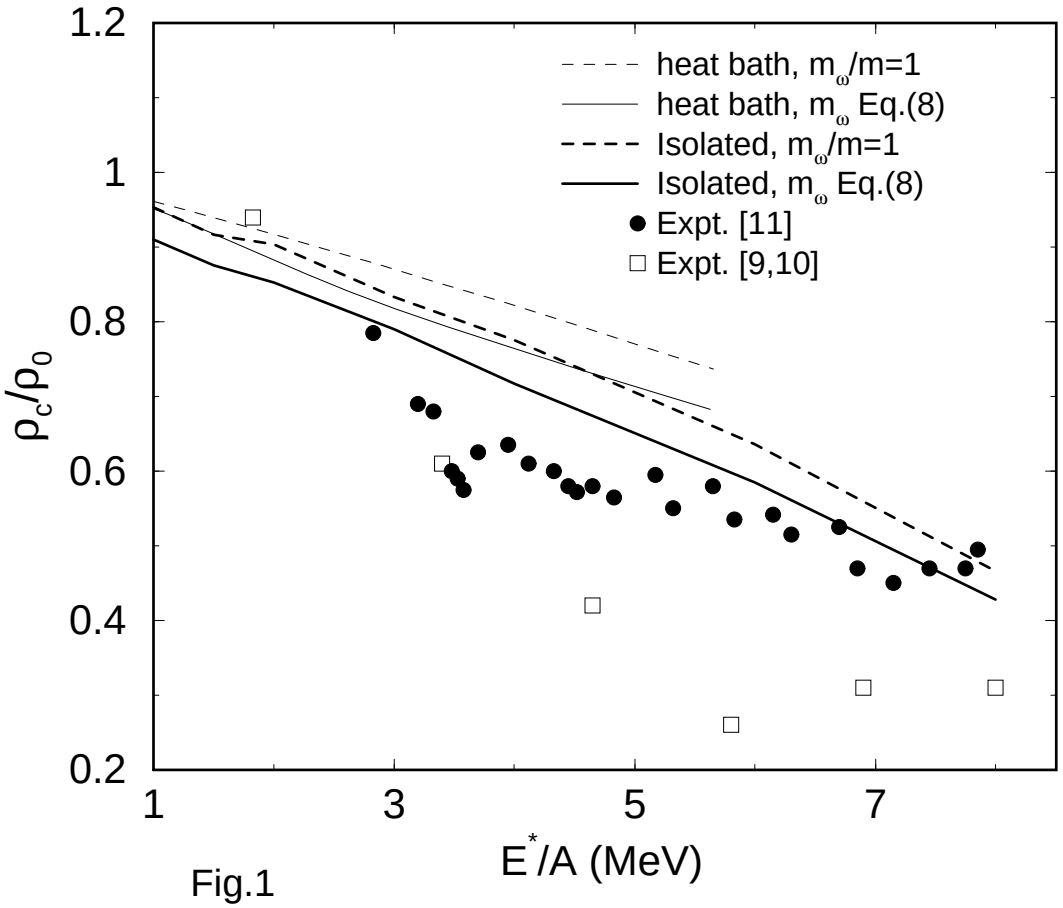
1.2
1
0.8
0.6
0.4
0.2
1
3
5
7
ρc/ρ0
E*/A (MeV)
heat bath, mω/m=1
heat bath, mω Eq.(8)
Isolated, mω/m=1
Isolated, mω Eq.(8)
Expt. [11]
Expt. [9,10]

Fig.1

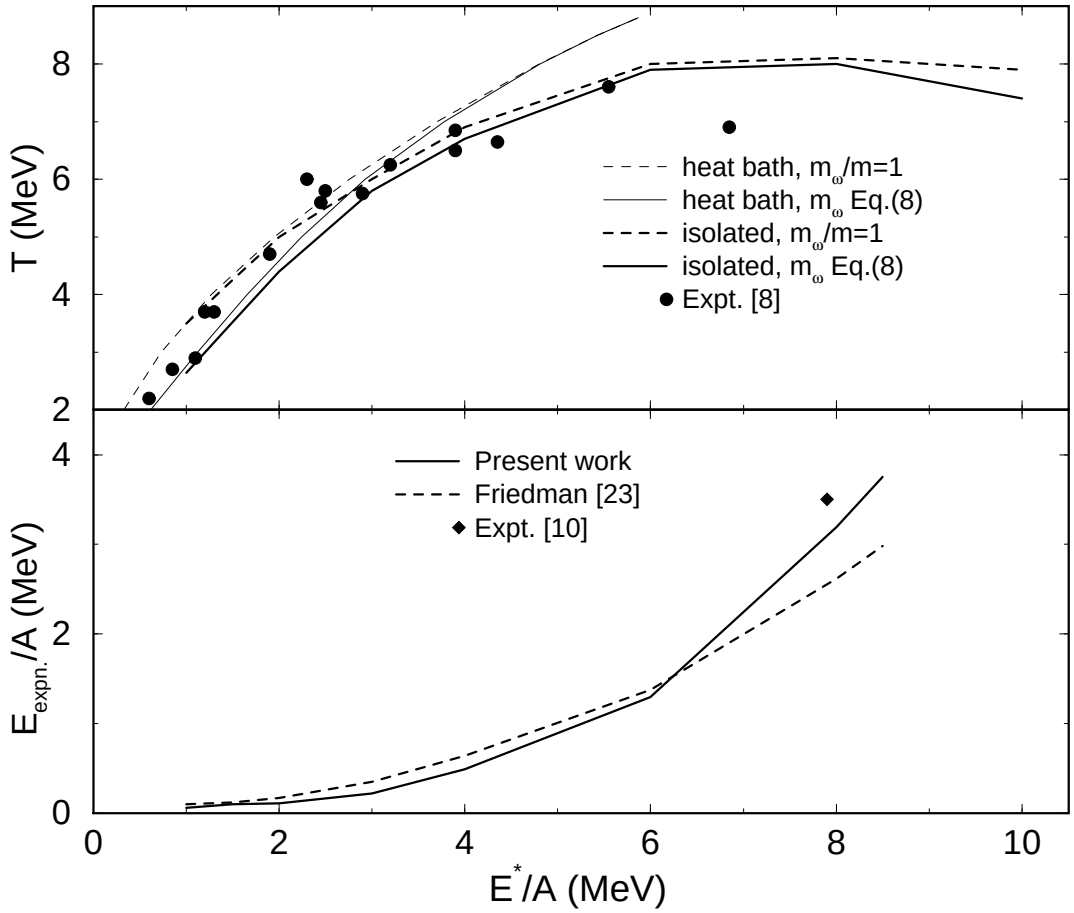
T (MeV)
heat bath, m_ω/m=1
heat bath, m_ω Eq.(8)
isolated, m_ω/m=1
isolated, m_ω Eq.(8)
Expt. [8]
$E_{expn.}/A$ (MeV)
Present work
Friedman [23]
Expt. [10]
E^*/A (MeV)

Fig.2

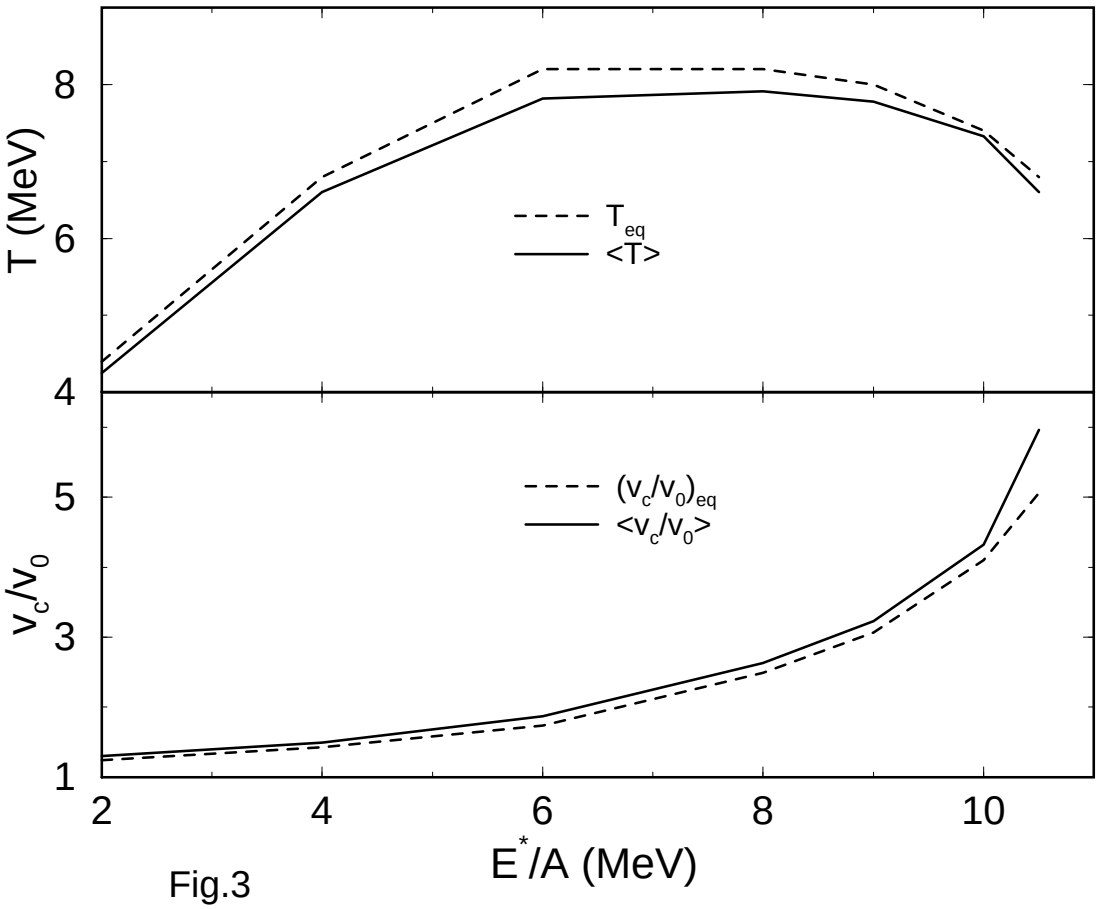

Fig.3

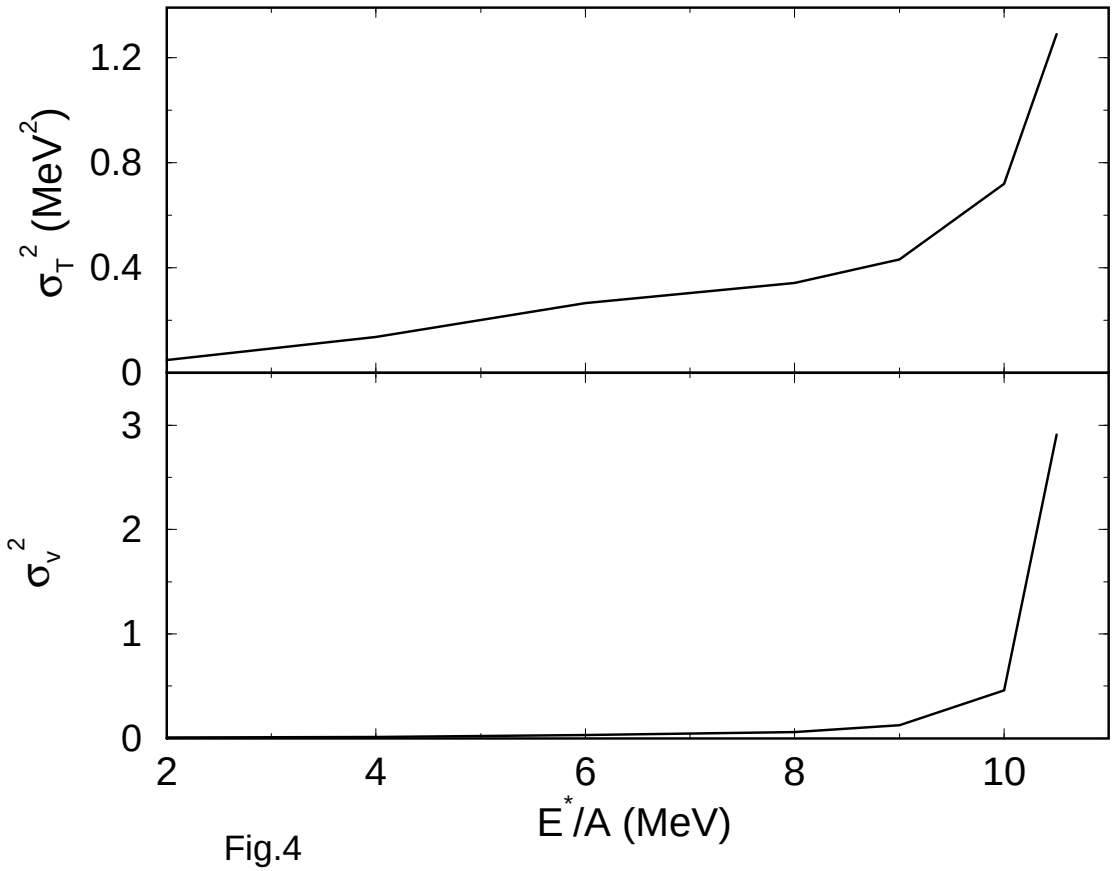

Fig.4

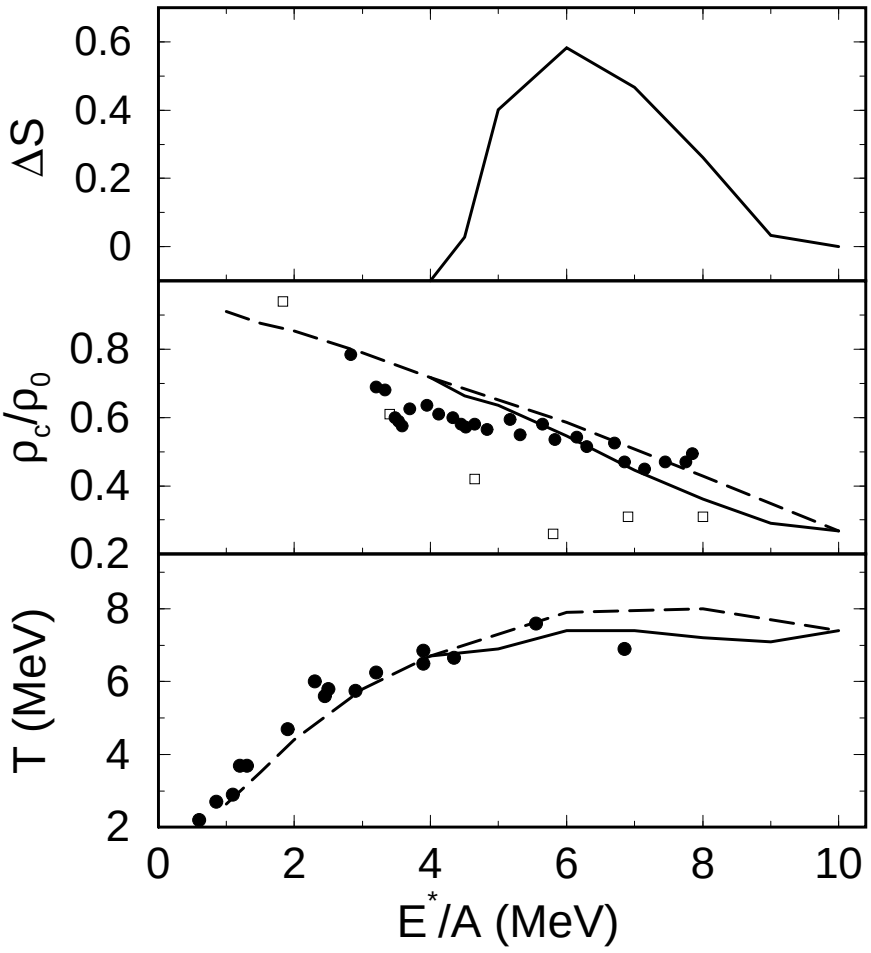

Fig.5